Voronoi tessellation of the packing of fine uniform spheres

R. Y. Yang, R. P. Zou, and A. B. Yu*
Center for Computer Simulation and Modelling of Particulate Systems, School of Materials Science and Engineering, The University of New South Wales, Sydney, NSW 2052, Australia
(Received 21 November 2001; published 3 April 2002)

The packing of uniform fine spherical particles ranging from 1 to 1000 μm has been simulated by means of discrete particle simulation. The packing structure is analyzed, facilitated by the well established Voronoi tessellation. The topological and metric properties of Voronoi polyhedra are quantified as a function of particle size and packing density. The results show that as particle size or packing density decreases, (i) the average face number of Voronoi polyhedra decreases, and the distributions of face number and edge number become broader and more asymmetric; (ii) the average perimeter and area of polyhedra increase, and the distributions of polyhedron surface area and volume become more flat and can be described by the log-normal distribution. The topological and metric properties depicted for the packing of fine particles differ either quantitatively or qualitatively from those reported in the literature although they all can be related to packing density. In particular, our results show that the average sphericity coefficient of Voronoi polyhedra varies with packing density, and although Aboav-Weaire's law is generally applicable, Lewis's law is not valid when packing density is low, which are contrary to the previous findings for other packing systems.

DOI: 10.1103/PhysRevE.65.041302 PACS number(s): 81.05.Rm, 61.43.Bn, 61.43.Gt, 81.20.Ev

I. INTRODUCTION

Fine particles ranging from 100 down to 0.1 μm are important to many industries, including mineral, materials, pharmaceutical, and chemical industries. For those particles, cohesive forces such as the van der Waals force and the electrostatic force are dominant [1,2]. Consequently, their packing behavior is quite different from that of coarse particles [3–5], and understanding of the underlying physics in terms of forces and structure is necessary in order to produce results of wide application. However, at present it is extremely difficult, if not impossible, to study experimentally the packing structure of fine particles and quantify directly the effect of the cohesive forces. Computer simulation has been an attractive alternative. This is particularly true in recent years because of the use of the so-called discrete element method (DEM) [6]. By this method, particle packing can be readily studied as a dynamic process, consistent with common practice in reality [7,8]. Recently, we successfully simulated the packing of fine particles by incorporating the van der Waals force into the DEM [9]. Our simulated relationship between packing density and particle size agrees well with that measured. We also analyzed the packing structures in terms of the commonly used structural parameters such as radial distribution function (RDF) and coordination number.

A further analysis of the packing structure can be achieved by quantifying the metric and topological properties of the Voronoi polyhedra [10] (also called Dirichlet cells in two dimensions [11]). Such analysis is very useful as it can provide information much richer than the one-dimensional (1D) RDF that has eliminated by averaging the three-dimensional nature of a packing of particles [12]. Since the work of Bernal [13] and Finney [14], the Voronoi tessellation has been widely accepted as a powerful tool to study the structure of disordered system. In fact, it has been directly used in the study of transport properties, e.g., effective thermal conductivity of porous media or composite solids [15–17]. The Voronoi tessellation has been extended to the packing of multisized spheres [18,19] or nonspherical particles [20]. Recently Oger *et al.* [21,22] performed a rather comprehensive investigation of the topological and metric properties of Voronoi polyhedra as a function of packing density. Their packings were built numerically through random sequential adsorption (RSA) and modified Powell algorithm where forces between particles were not considered.

In this paper, we apply the Voronoi tessellation to analyze the packings of fine particles ranging from 1 to 1000 μm. Different from Oger *et al.* [21,22], our packings are generated by means of a DEM-based model and hence more related to the packing of fine particles in reality. We quantify the topological and metric properties of Voronoi polyhedra and their variation with particle size or packing density.

II. SIMULATION METHOD

A packing is constructed through DEM in which the motion of individual particles and their interaction with each other are traced [6,9]. This motion is governed by the contact forces, the van der Waals force, and the gravity, as illustrated schematically in Fig. 1. The displacement of particle i of radius R_i and mass m_i in a time step can be computed based on Newton's second law of motion given by

$$m_i \frac{d\mathbf{v}_i}{dt} = \sum_j (\mathbf{F}_{ij}^n + \mathbf{F}_{ij}^s + \mathbf{F}_{ij}^v) + m_i \mathbf{g} \tag{1}$$

and

$$I_i \frac{d\boldsymbol{\omega}_i}{dt} = \sum_j (\mathbf{R}_i \times \mathbf{F}_{ij}^s - \mu_r R_i |\mathbf{F}_{ij}^n| \hat{\boldsymbol{\omega}}_i), \tag{2}$$

*Corresponding author. FAX: +61-2-9385-5956; email address: a.yu@unsw.edu.au

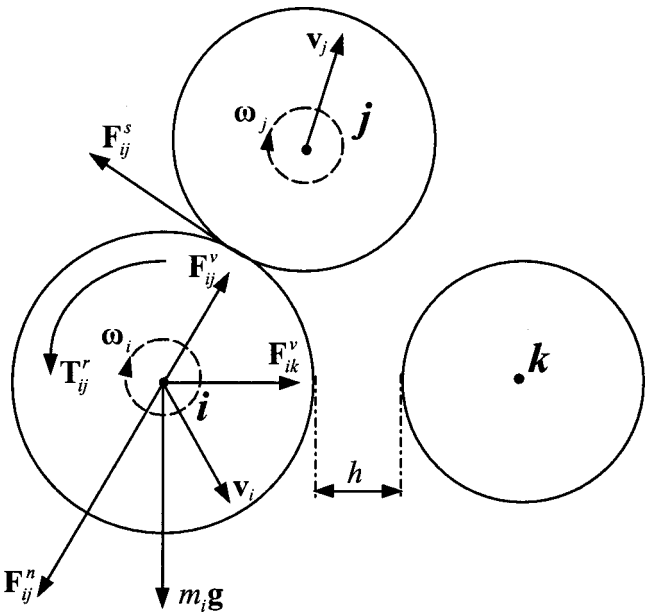

FIG. 1. Schematic illustration of the forces acting on particle *i* from contacting particle *j* and noncontacting particle *k*.

where $\mathbf{v}_i$, $\boldsymbol{\omega}_i$, and I_i are, respectively, the translational and angular velocities, and the moment of inertial of particle *i*; $\mathbf{F}_{ij}^n$, $\mathbf{F}_{ij}^s$, and $\mathbf{F}_{ij}^v$ represent, respectively, the normal contact force, the tangential contact force, and the van der Waals force imposed on particle *i* by particle *j*. The first part of the right-hand side in Eq. (2) is the torque due to the tangential force $\mathbf{F}_{ij}^s$, where $\mathbf{R}_i$ is a vector running from the center of the particle to the contact point with its magnitude equal to particle radius R_i. The second part is the rolling friction torque $\mathbf{T}_{ij}^r$ arising from the elastic hysteresis loss and time-dependent viscous dissipation [23,24], and μ_r is the coefficient of rolling friction. This friction resistance has been demonstrated to play a critical role in achieving physically or numerically stable sandpile, viz. the unconfined packing of particles [25]. Table I gives equations used to calculate the forces. More detail can be found from our previous paper [9].

A packing was formed with 5000 particles in a rectangular box of width 15 particles in diameter, larger than the box of width 10 particles diameter used in our previous work [9] to improve the accuracy and statistical reliability of the resulting Voronoi polyhedra. Periodical boundary conditions were applied along two horizontal directions to avoid the lateral wall effect. The simulation was started with particles dispersing homogeneously without overlap in the box. Then, the particles were allowed to settle down under gravity and during this densification process, they would collide with neighboring particles and bounce upward or downward. This dynamic process ended when all particles reached their stable positions with an essentially zero velocity as a result of the damping effect for energy dissipation. This packing process is equivalent to a physical operation to transform a fluidized bed to a fixed bed by stopping gas supply. The simulations were performed for monosized particles, with their diameters ranging from 1 to 1000 μm. Totally, seven packings were used for the present analysis as listed in Table II.

III. RESULTS AND DISCUSSION

We considered the following properties resulting from the Voronoi tessellation.

(a) Number of edges for each polyhedron face.
(b) Number of faces for each polyhedron.
(c) Perimeter and area of a polyhedron face.
(d) Perimeter, area and volume of a polyhedron.

The former two properties are known as typical topological properties and the latter two are the most widely used metric properties. These properties are distributed variables, as a natural consequence of disordered packing structure for each sized particles. The following discussion will focus on how these properties vary with particle size *d* or packing density *C*.

A. Topological properties

Figure 2 shows the percentage of polyhedra with *f* faces for different sized particles. For the packing of 1000 μm particles ($C=0.605$), the distribution is almost symmetric with $f=14$ being the most prevailing value. Significant contribution also comes from $f=13$ and 15. This is consistent with the previous experimental and numerical studies of the packing of hard spheres [14,21,29]. When particle size or packing density decreases, the distribution becomes broader and more asymmetric. The percentage of polyhedra with 12 faces remains a constant (around 7%) for all the packings, consistent with the previous study [30].

TABLE I. Summary of forces acting on particle *i* from particle *j*. In these equations $E=Y/(1-\tilde{\sigma}^2)$, $\overline{R}=R_iR_j/(R_i+R_j)$, $\xi_{s,\max}=\mu_s[(2-\tilde{\sigma})/2(1-\tilde{\sigma})]\xi_n$ [28], $h=\max(h,h_{\min})$, Y is Young's modulus, $\tilde{\sigma}$ is the Poisson ratio, $\hat{\mathbf{n}}_{ij}=(\mathbf{R}_i-\mathbf{R}_j)/|\mathbf{R}_i-\mathbf{R}_j|$, γ_n is the normal damping coefficient, μ_s is the sliding friction coefficient, ξ_s is the total tangential displacement, H_a is the Hamaker constant, and $h_{\min}$ is the minimum gap.

Force	Symbol	Equation	Reference
Normal force	$\mathbf{F}_{ij}^n$	$[\frac{2}{3}E\sqrt{\overline{R}}\xi_n^{3/2}-\gamma_nE\sqrt{\overline{R}}\sqrt{\xi_n}(\mathbf{v}_{ij}\cdot\hat{\mathbf{n}}_{ij})]\overline{\mathbf{n}}_{ij}$	[24]
Tangential force	$\mathbf{F}_{ij}^s$	$-\mathrm{sgn}(\xi_s)\mu_s\lvert\mathbf{F}_{ij}^n\rvert\{1-[1-\min(\xi_s,\xi_{s,\max})/\xi_{s,\max}]\}$	[26]
van der Waals force	$\mathbf{F}_{ij}^v$	$-\frac{H_a}{6}\frac{64R_i^3R_j^3(h+R_i+R_j)}{(h^2+2R_ih+2R_jh)^2(h^2+2R_ih+2R_jh+4R_iR_j)^2}\hat{\mathbf{n}}_{ij}$	[2,27]

TABLE II. Averaged topological and metric properties of Voronoi polyhedra.

Size (μm)	Packing density	Edge numbers per face[a]	Face numbers per polyhedron	Perimeter of polyhedron	Area of polyhedron	Volume of polyhedron
1	0.188	5.217	15.33	35.63	12.49	3.102
5	0.341	5.211	15.20	20.08	7.82	1.593
10	0.427	5.201	15.01	18.33	6.58	1.256
20	0.469	5.197	14.94	17.62	6.09	1.131
50	0.519	5.191	14.84	16.84	5.61	1.009
100	0.573	5.177	14.58	16.11	5.17	0.913
1000	0.605	5.167	14.41	15.72	4.95	0.865

[a]The perimeter and area of face can be derived from the perimeter and area of the polyhedron.

Figure 3 shows the percentage of faces with e edges as a function of packing density. Parallel to the variation of the face distribution in Fig. 2, the edge distribution also becomes broader and more asymmetric when packing density decreases. Vertices in the Voronoi construction represent the intersection of four Voronoi polyhedra (in random configurations). By the Euler relation, the average number of faces per polyhedron $\langle f \rangle$ and the average number of edges per polyhedron face $\langle e \rangle$ are linked [31]:

$$\langle e \rangle = 6 - 12/\langle f \rangle. \tag{3}$$

The data listed in Table II confirm that our results strictly obey this relation. Therefore, either $\langle e \rangle$ or $\langle f \rangle$ alone can be used in a quantitative analysis. Figure 4 shows $\langle f \rangle$ as a function of packing density, indicating $\langle f \rangle$ increases as packing density decreases. The results reported in the literature are also plotted for comparison, showing our results agree quite well with those obtained by Finney [14] and Jullien *et al.* [32]. Note that our results also agree with those obtained from the so-called Powell packing [22], but are consistently higher than the results obtained by Oger *et al.* [22] using the RSA algorithm and spatial dilution of the Powell packing.

Different simulation algorithms represent different mechanisms of forming a packing and hence generate different results. Oger *et al.* [22] used both RSA algorithm and molecular dynamics (MD) simulation to generate packings with different packing densities. RSA packing is built sequentially with the simple rule that the next particle, whose center is chosen at random, should not overlap the previous ones. This algorithm can only generate packing with packing density up to 0.38 [33]. To obtain a homogenous packing of higher packing density, Oger *et al.* [22] adopted the MD simulation where an initial packing is built using Powell algorithm, followed by ''thermal'' expansion. The particles in the resulting packing are not touching and such a packing is therefore ''nonstable'' under external forces. On the other hand, the Powell packing [34] is built sequentially by adding particle by choosing the site nearest to a plane surface, in contact with three particles already placed. This model simulates the packing under gravity and is anisotropic. The results of Jullien *et al.* [32] were obtained with the Jodrey-Tory (JT) algorithm [35], which is a collective algorithm. The JT simulation starts with a random distribution of points with inner and outer radii. The inner radius defines the true density and the outer a nominal density. By moving the position of points and shrinking the outer radius, the overlaps among particles are gradually eliminated. The final packing is formed when the true density equals the nominal density, and its structure is isotropic [32].

Obviously, the above algorithms are largely developed from geometrical consideration and cannot simulate the dy-

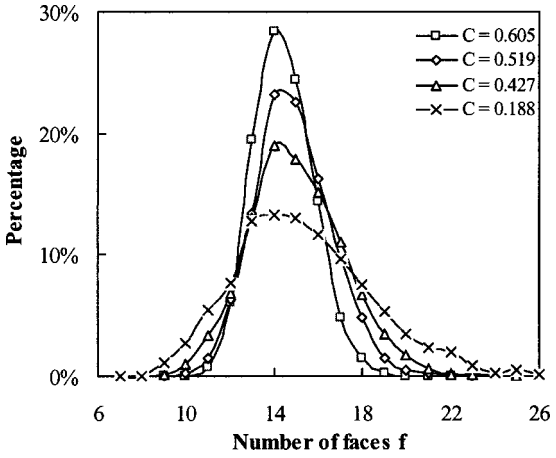

FIG. 2. The distribution of number of faces per polyhedron as a function of packing density C.

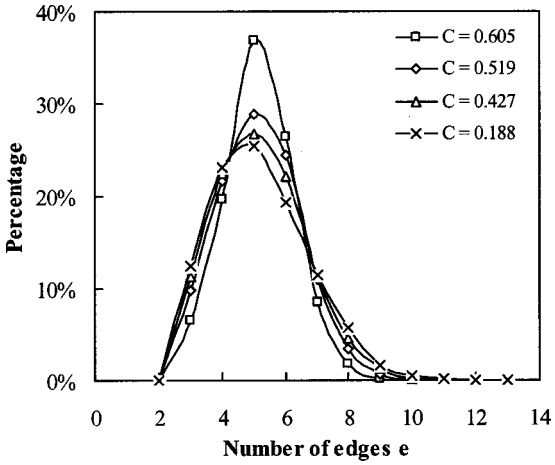

FIG. 3. The distribution of number of edges per face as a function of packing density C.

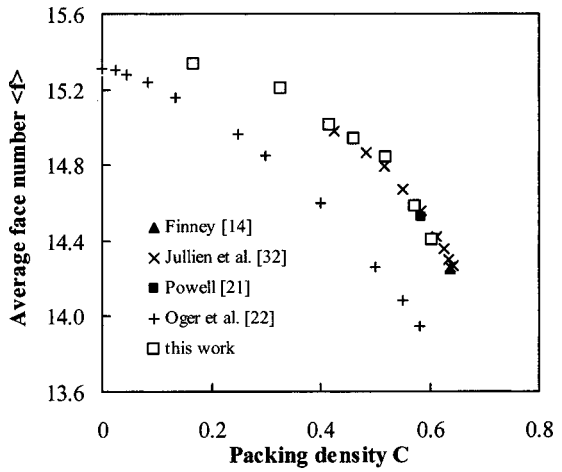

FIG. 4. Variation of average face number of Voronoi polyhedra with packing density.

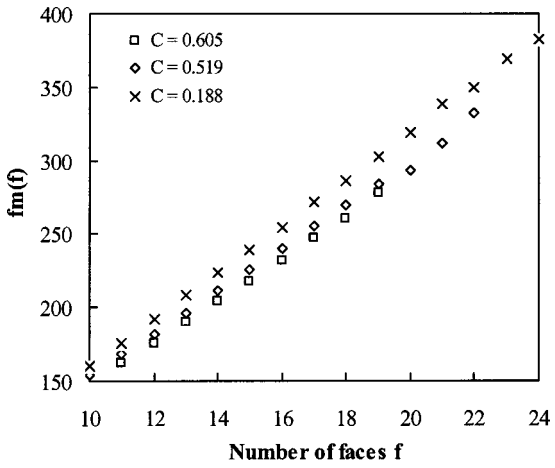

FIG. 5. Equation (4) applied to the packings with different packing density.

namic process of a packing in reality. This problem can be overcome by DEM, which considers not only the gravity but also the forces associated with granular materials. In fact, the present DEM simulation is specific to fine particles packed under gravity. Therefore, different from the other simulation algorithms, its packing density corresponds to particle size, a real physical parameter, not simply the stage of simulation. As shown elsewhere [9], the change of particle size actually represents the relative importance between the cohesive van der Waals force and the gravity. For coarse particles, the gravity is dominant and the packing density is 0.605, the typical poured packing density under the gravity. Gentle vibrating/tapping would increase packing density to 0.64, as measured by Finney [14]. Therefore, it is not surprising that the present results are comparable to those obtained with the gravity as the dominant force but different from the results from Oger *et al.* [22].

Aboav-Weaire's law, which was first proposed by Aboav [36] with the original aim of understanding the mechanism of the growth of polycrystals, describes the correlation between neighboring polyhedra, given by

$$fm(f)=(\langle f\rangle-a)f+\langle f\rangle a+\mu_2, \tag{4}$$

where $\mu_2(=\langle f^2\rangle-\langle f\rangle^2)$ is the second moment of the distribution of f, $m(f)$ is the average number of faces in neighboring polyhedra, and a is the only unknown parameter in the equation. This law has been found to be valid for various 2D packings [37] and can be predicted from maximum entropy arguments [38]. There are also a few reports of 3D networks to which this law is approximately applicable [39–41]. It can be seen from Fig. 5 that Aboav-Weaire's law is also applicable to every packing in the present work. Figure 6 shows the values of μ_2 and a as a function of packing density. It is evident that as μ_2 increases, a decreases, which is in agreement with the suggestion of Le Caër and Delannay [42]. In fact, Godrèche *et al.* [43] has reported that $\mu_2=10.5$ and $a\approx-1$ for their packing, which is largely arbitrarily built. It appears that their value is well connected with the present correlation between μ_2 and a, based on the packing results of fine particles. It is also interesting to note that when packing density increases from 0.573 to 0.605, there is a sudden drop in parameter a.

B. Metric properties

In this section, we investigate the variation of metric properties of Voronoi polyhedra, such as face perimeter (L), face area (A), polyhedron perimeter (P), polyhedron surface area (S), and polyhedron volume (V), with packing density C. For each property x, we consider its distribution and average value $\langle x\rangle$. For the purpose of comparison, all distributions are represented in terms of $x^*(=x/\langle x\rangle)$, the reduced metric element with its average value as a reference. The applicability of Lewis's and Desch's law [44] will also be examined.

Figure 7 shows the results for face area. It is obvious from Fig. 7(a) that the average face area $\langle A\rangle$ decreases with packing density, approximately proportional to $C^{-2/3}$. There are two peaks in the distribution of face areas for a packing [Fig. 7(b)]. The first one is very strong and realized when A^*

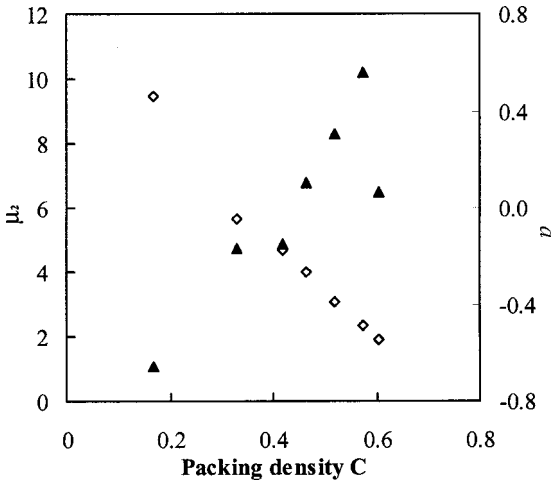

FIG. 6. Parameters μ_2 (◇) and a (▲) in Aboav-Weaire's law as a function of packing density.

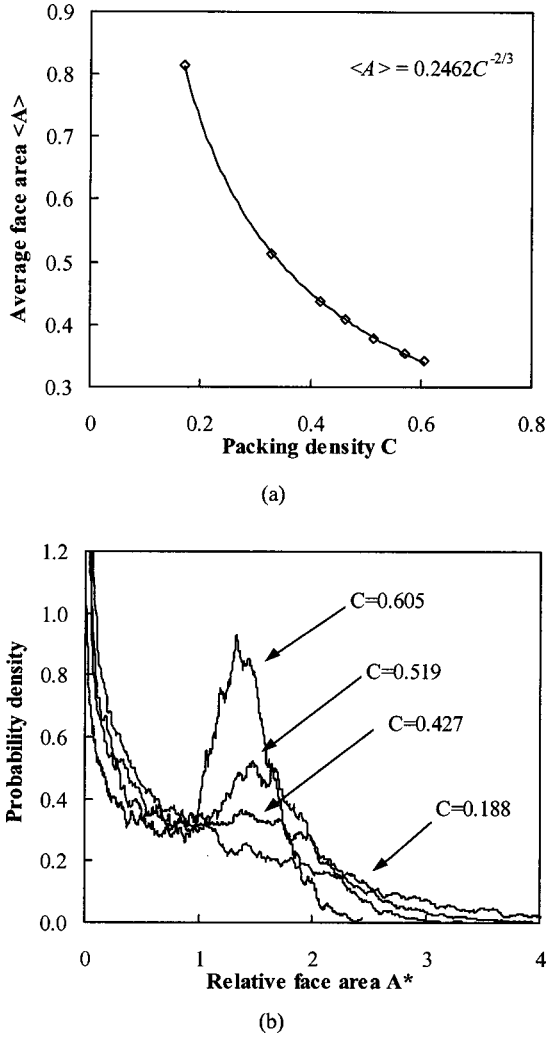

FIG. 7. Face area of Voronoi polyhedra as a function of packing density C. (a) Average face area (units of d^2); (b) probability density distribution.

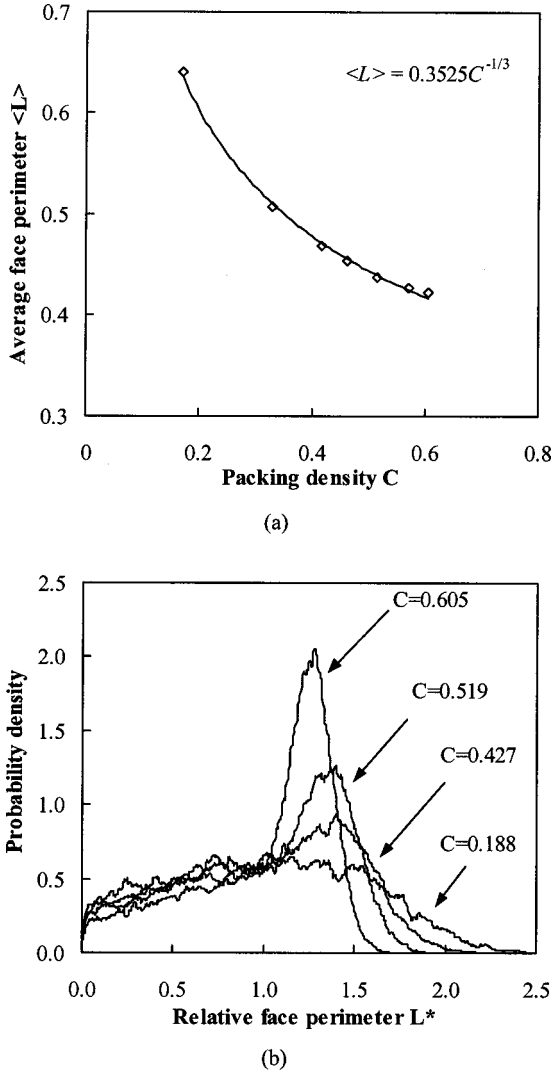

FIG. 8. Face perimeter of Voronoi polyhedra as a function of packing density C. (a) Average face perimeter (units of d); (b) probability density distribution.

tends to zero. The second one is obtained at a higher value of face area and varies with C. In particular, this peak shifts slightly towards higher face areas and gradually flattens out as the packing density decreases. For the packing of 1 μm particles ($C=0.188$), the peak vanishes completely. Figure 8 shows that the average face perimeter decreases with packing density, where $L \propto C^{-1/3}$. Unlike the face area distribution, the face perimeter distribution has only one strong peak that becomes weaker and shifts slightly towards a higher face perimeter as packing density decreases.

The change of the distribution of face area or perimeter results from the change of proportion of ''touching'' particles [45]. The area and perimeter of a Voronoi face between two touching particles must be greater than a certain minimum value because of the physical constraint that two particles cannot overlap. As packing density decreases the number of touching particles (coordination number) decreases [9]. This causes a decrease in the height of the second peak in the face area distribution and the peak in the face perimeter distribution. On the other hand, the loose open-tree structure of fine particles gives large face areas and hence an increased average face area and perimeter, as observed in Figs. 7 and 8.

By definition, the average volume of polyhedra $\langle V \rangle$ is inversely proportional to packing density C, i.e., $\langle V \rangle = (1/6)\pi d^3/C$. The present results suggest that the average perimeter $\langle P \rangle$ and surface area $\langle S \rangle$ of polyhedra are, respectively, proportional to $C^{-1/3}$ and $C^{-2/3}$, as shown in Fig. 9. This relationship was also found by Oger *et al.* [21] for their packing. However, as discussed above, the previous and present results are quantitatively different as they are corresponding to different physical systems.

Two parameters have been found to be useful in relating these average values, given by

$$K_1 = \frac{36\pi \langle V \rangle^2}{\langle S \rangle^3} \tag{5}$$

and

$$K_2 = \frac{1}{3}\left(\frac{4\pi}{3}\right)^{2/3} \frac{\langle P \rangle}{\langle V \rangle^{1/3}}, \tag{6}$$

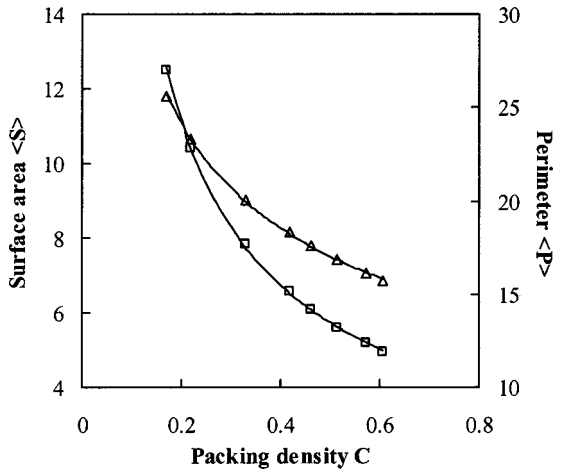

FIG. 9. Average surface area $\langle S\rangle$ (□, units of d^2) and perimeter $\langle P\rangle$ (△, units of d) as a function of packing density C. The lines are, respectively, given by $\langle S\rangle = 4.0078C^{-2/3} - 0.6232$ and $\langle P\rangle = 15.699C^{-1/3} - 2.7488$.

K_1 is known as the sphericity coefficient of a polyhedron, and $K_2C^{-2/3}$ is the average length per unit volume [46]. For the RSA packings, Oger *et al.* [21] found that K_1 and K_2 are independent of packing density and approximately equal to about 0.75 and 14.3, respectively. However, our results show that both K_1 and K_2 vary with packing density. As shown in Fig. 10, K_1 increases and K_2 decreases with packing density. Our results are consistent with those obtained by Jodrey and Tary [35] who focused on the K_1-C relation, and well connected with the face-centered cubic (fcc) packing, the theoretical maximum packing for monosized spheres. This trend indicates that as packing density or particle size decreases, the average shape of polyhedron in a packing is less spherical.

Figures 11 and 12 show the distributions of the reduced polyhedron surface S^* and volume V^*. Both distributions become wider when particle size or packing density decreases. However, it is found that the peak value of the volume distribution shifts more substantially to lower volumes than that of the area distribution and the whole curve becomes more asymmetric with a quite long tail. As pointed out by Montoro and Abascal [12], the asymmetry observed is a consequence of the fact that there is no upper limit for the maximum area or volume of a polyhedron, conversely, there is a lower limit because the area or volume of each polyhedron must be larger than a certain value to contain a particle.

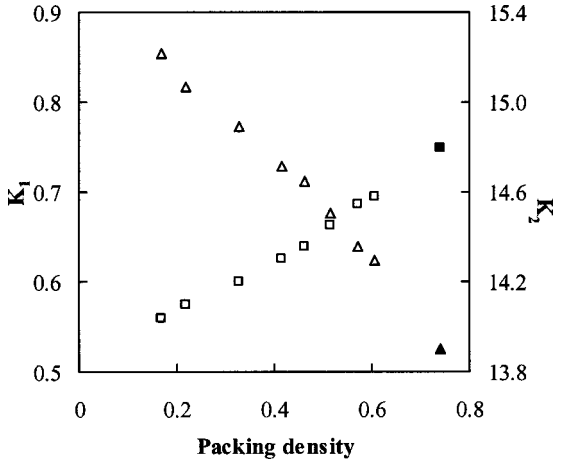

FIG. 10. Dimensionless ratios K_1 (□) and K_2 (△) as a function of packing density C, where ■ and ▲ correspond to the fcc packing.

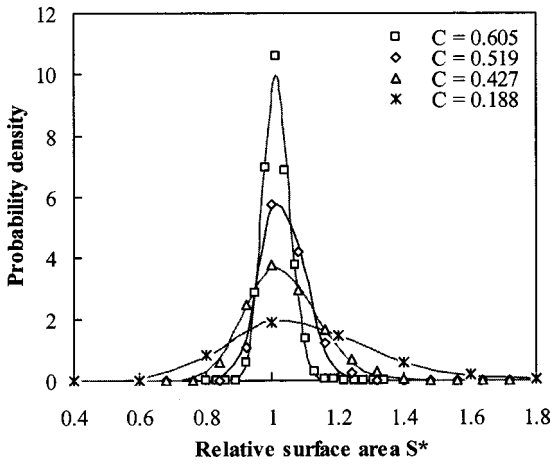

FIG. 11. The relative area distribution of Voronoi polyhedra as a function of packing density C; lines are the results from Eq. (7).

For quantitative and general application, in the past various attempts have been made to fit the distribution of area and volume of polyhedra using statistical distributions, such as Gaussian, Gamma, and Maxwell distributions [21,47–49]. These distributions are either too complicated or unable to provide satisfactory results. As shown in Figs. 11 and 12, both the area and volume distributions can be well described by the log-normal distribution, given by

$$f(x^*) = \frac{1}{\sqrt{2\pi}(x^* - x^*_{\min})\sigma} \exp\{-[\ln(x^* - x^*_{\min}) - \mu]^2/2\sigma^2\}, \tag{7}$$

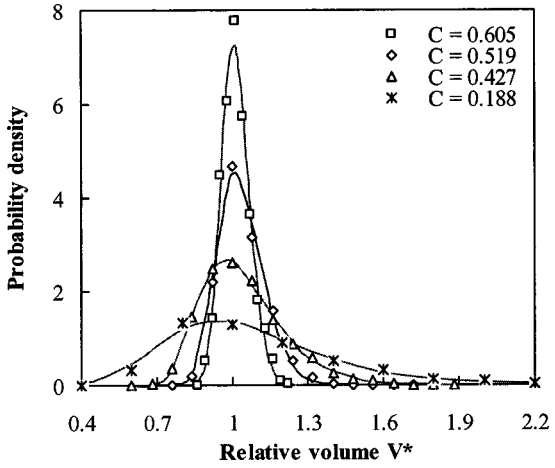

FIG. 12. The relative volume distribution of Voronoi polyhedra as a function of packing density C; lines are the results from Eq. (7).

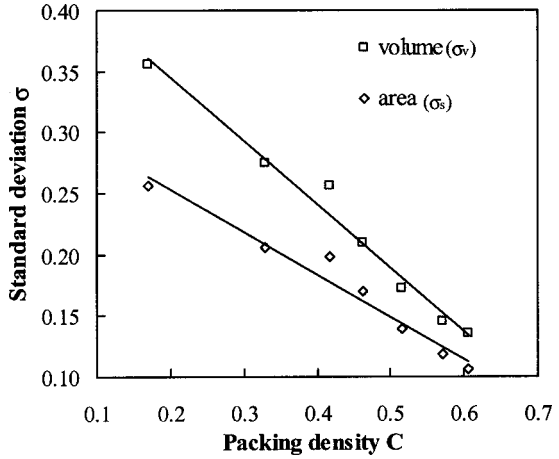

FIG. 13. Standard deviation σ in Eq. (7) as a function of packing density. The lines are, respectively, given by $\sigma_s = -0.3469C + 0.3226$ and $\sigma_v = -0.5193C + 0.4489$.

where $x^*_{\min}$, as the lower limit, is assumed to correspond to the surface area (πd^2) or volume ($\pi d^3/6$) of a sphere, μ is theoretically related to the mean value $\langle x \rangle$ and standard deviation σ [50], here given by $\mu = \ln(\langle x \rangle - x_{\min}) - \ln(\langle x \rangle) - \sigma^2/2$. Both $\langle S \rangle$ and $\langle V \rangle$ can be calculated from the knowledge of C. Figure 13 shows that σ also varies with C, described by a simple linear equation. Therefore, for fine particles, the area and volume distributions of Voronoi polyhedra can be well treated as a function of a single variable, i.e., packing density C.

Lewis's law [51] and Desch's law [52] are two empirical relations which state that (in three dimensions) the average volume V_f and surface area S_f of f faced Voronoi polyhedra each vary linearly with f, given, respectively, by

$$V_f = 1 + \frac{f - \langle f \rangle}{K_v} \tag{8}$$

and

$$S_f = 1 + \frac{f - \langle f \rangle}{K_s}, \tag{9}$$

where K_v and K_s are parameters dependent on packing density [22]. The two empirical laws have been observed in many cellular networks [37,53–55]. Oger *et al.* [21] have shown that the two equations are also applicable to their RSA packings. Rivier and Lissowski [56] tried to use the maximum entropy method to show these linear relationships maximize the entropy under some constraints. However, as pointed out by Chiu [57], this maximum entropy approach cannot derive or prove these laws. Actually, Drouffe and Itzykson [54] showed that in 2D Lewis's law is no more valid when the number of edges $e > 12$. The present results indicate that the above equations are only valid for larger particles with higher packing density ($d > 50$ μm, $C > 0.5$), as shown in Fig. 14. When particle diameter is less than 10 μm ($C = 0.427$), significant deviation from linearity can be found. Fortes [41] reported that Lewis's law is exact when Aboav-Weaire's law is exact. However, the present study shows an opposite: Lewis's law is not always valid even when Aboav-Weaire's law is applicable.

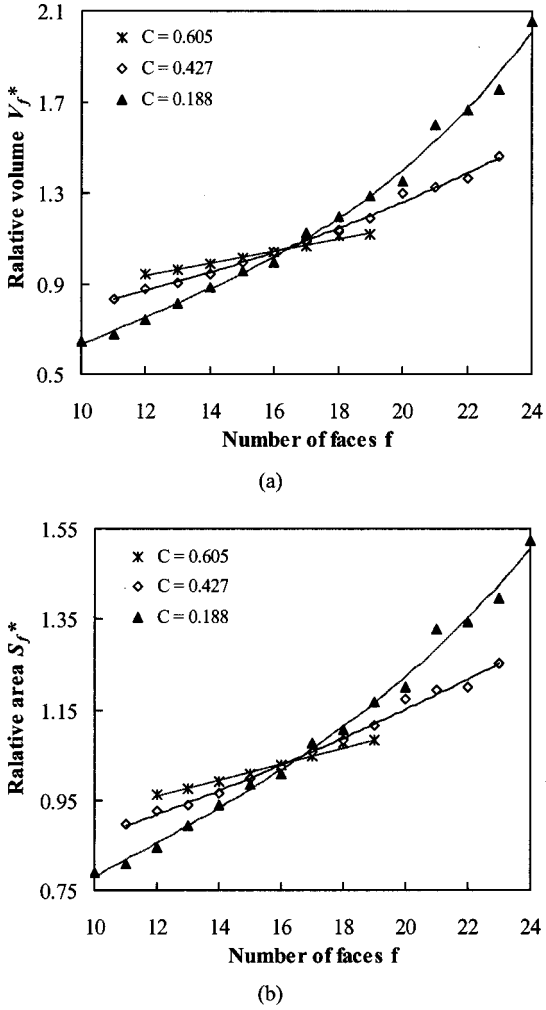

FIG. 14. The relationship between (a) the volume and (b) the area of f-faced polyhedra and the number of faces for packings with different packing densities C.

IV. CONCLUSIONS

We have reported the results of the statistics of Voronoi polyhedron for the packing of fine particles, simulated by a DEM-based algorithm. Typical topological and metric properties have been quantified as a function of particle size or packing density. Our results show the following.

(1) As packing density or particle size decreases, (a) the average face number of Voronoi polyhedra decreases, the distributions of face number and edge number become broader and more asymmetric; (b) the average perimeter and area of polyhedra increase and the distributions of polyhedron surface area and volume become more flat. Both distributions can be described by the log-normal distribution whose parameters can all be related to packing density; (c) geometric ratios K_1 and K_2, given by Eqs. (5) and (6), decreases and increases, respectively.

(2) Different simulation algorithms represent different mechanisms of forming a packing of particles, and hence different physical packing systems. Consequently, the topological and metric properties depicted for the packing of fine particles quantitatively differ from those reported in the literature for other packing systems although they all can be related to packing density. Conflicting results can also be observed. For example, contrary to the results of Oger *et al.* [21,22], the present results show that K_1 and K_2 vary with packing density; against the findings of Oger *et al.* [21,22] and Fortes [41], although Aboav-Weaire's law is generally applicable to fine particles, Lewis's law is not valid when packing density is low.

ACKNOWLEDGMENT

The authors are grateful to ARC (Australian Research Council) for financial support of this work.

[1] J. Visser, Powder Technol. **58**, 1 (1989).
[2] J. N. Israelachvili, *Intermolecular & Surface Forces*, 2nd ed. (Academic Press, London, 1991).
[3] J. V. Milewski, in *Handbook of Fillers and Reinforcements For Plastics*, edited by H. S. Kata and J. V. Milewski, 2nd ed. (Van Nostrand Reinhold, New York, 1987).
[4] R. M. German, *Particle Packing Characeristics* (Metal Powder Industries Federation, Princeton, NJ, 1989).
[5] A. B. Yu, J. Bridgwater, and A. Burbidge, Powder Technol. **92**, 185 (1997).
[6] P. A. Cundall and O. D. L. Stack, Geotechnique **29**, 47 (1979).
[7] L. F. Liu, Z. P. Zhang, and A. B. Yu, Physica A **268**, 433 (1999).
[8] Z. P. Zhang, L. F. Liu, Y. Y. D., and A. B. Yu, Powder Technol. **116**, 23 (2001).
[9] R. Y. Yang, R. P. Zou, and A. B. Yu, Phys. Rev. E **62**, 3900 (2000).
[10] G. F. Voronoi, J. Reine Angew. Math. **134**, 198 (1908).
[11] G. L. Dirichlet, J. Reine Angew. Math. **40**, 216 (1850).
[12] J. C. G. Montoro and J. L. F. Abascal, J. Phys. Chem. **97**, 4211 (1993).
[13] J. D. Bernal, Proc. R. Soc. London, Ser. A **280**, 299 (1964).
[14] J. L. Finney, Proc. R. Soc. London, Ser. A **319**, 479 (1970).
[15] M. Kobayashi, H. Maekawa, H. Nakamura, and Y. Kondou, Trans. Jpn. Soc. Mech. Eng. **537**, 1795 (1991).
[16] M. Sahimi and T. T. Tsotsis, Ind. Eng. Chem. Res. **36**, 3043 (1997).
[17] G. J. Cheng, A. B. Yu, and P. Zulli, Chem. Eng. Sci. **54**, 4199 (1999).
[18] B. J. Gellatly and J. L. Finney, J. Non-Cryst. Solids **50**, 313 (1982).
[19] P. Richard, L. Oger, J. P. Troadec, and A. Gervois, Physica A **259**, 205 (1998).
[20] V. A. Luchnikov, N. N. Medvedev, L. Oger, and J.-P. Troadec, Phys. Rev. E **59**, 7205 (1999).
[21] L. Oger, A. Gervois, J. P. Troadec, and N. Rivier, Philos. Mag. B **74**, 177 (1996).
[22] L. Oger, J. P. Troadec, P. Richard, A. Gernois, and N. Rivier, *Powder & Grains* (Balkema, Rotterdam, 1997) p. 287.
[23] D. Tabor, Proc. R. Soc. London, Ser. A **229**, 198 (1955).
[24] N. V. Brilliantov, F. Spahn, J. M. Hertzsch, and T. Pöschel, Phys. Rev. E **53**, 5382 (1996).
[25] Y. C. Zhou, B. D. Wright, R. Y. Yang, B. H. Xu, and A. B. Yu, Physica A **269**, 536 (1999).
[26] R. D. Mindlin and H. Deresiewicz, J. Appl. Mech. **20**, 327 (1953).
[27] H. C. Hamaker, Physica (Amsterdam) **58**, 1058 (1937).
[28] P. A. Langston, U. Tüzün, and D. M. Heyes, Chem. Eng. Sci. **50**, 967 (1995).
[29] N. D. Aparicio and A. C. F. Cocks, Acta Metall. Mater. **43**, 3873 (1995).
[30] R. Jullien, A. Pavlovitch, and P. Meaking, J. Phys. A **25**, 4103 (1992).
[31] N. Rivier, in *Disorder and Granular Media*, edited by D. Bideau and A. Hansen (Elsevier Science Publishers, Amsterdam, 1993).
[32] R. Jullien, P. Jund, D. Caprion, and D. Quitmann, Phys. Rev. E **54**, 6035 (1996).
[33] D. W. Cooper, Phys. Rev. A **38**, 522 (1988).
[34] M. J. Powell, Powder Technol. **25**, 45 (1980).
[35] W. S. Jodrey and E. M. Tory, Phys. Rev. A **32**, 2347 (1985).
[36] D. A. Aboav, Metallography **3**, 383 (1970).
[37] S. N. Chiu, Mater. Charact. **34**, 149 (1995).
[38] M. A. Peshkin, K. J. Strandburg, and N. Rivier, Phys. Rev. Lett. **67**, 1803 (1991).
[39] M. A. Fortes, J. Phys. (Paris) **50**, 725 (1989).
[40] M. A. Fortes, Philos. Mag. Lett. **68**, 69 (1993).
[41] M. A. Fortes, J. Phys. A **28**, 1055 (1995).
[42] G. Le Caër and R. Delannay, J. Phys. A **26**, 3931 (1993).
[43] C. Godrèche, I. Kostov, and I. Yekutieli, Phys. Rev. Lett. **69**, 2674 (1992).
[44] C. H. Desch, J. Inst. Met. **22**, 241 (1919).
[45] P. L. Spedding and R. M. Spencer, Comput. Chem. Eng. **22**, 247 (1998).
[46] J. L. Meijering, Philips Res. Rep. **8**, 270 (1953).
[47] T. Kiang, Z. Astrophys. **64**, 433 (1966).
[48] H. G. Hanson, J. Stat. Phys. **30**, 591 (1983).
[49] D. Weaire, J. P. Kermode, and J. Wejchert, Philos. Mag. B **53**, L101 (1986).
[50] J. Aitchison and J. A. C. Brown, *The Lognormal Distribution: With Special Reference to its Uses in Economics* (Cambridge University Press, Cambridge, 1957).
[51] F. T. Lewis, Anat. Rec. **38**, 341 (1928).
[52] N. Rivier, Philos. Mag. B **52**, 795 (1985).
[53] G. L. Caer and J. S. Ho, J. Phys. A **23**, 3279 (1990).
[54] I. M. Drouffe and C. Itzykson, Nucl. Phys. B **235**, 45 (1984).
[55] M. P. Quine and D. F. Watson, J. Appl. Probab. **21**, 548 (1984).
[56] N. Rivier and A. Lissowski, J. Phys. A **15**, L143 (1982).
[57] S. N. Chiu, J. Phys. A **28**, 607 (1995).